*J. Fluid Mech.* (1974), *vol.* 64, *part* 2, *pp.* 393–414
*Printed in Great Britain*



# Radiation properties of the semi-infinite vortex sheet: the initial-value problem

By D. G. CRIGHTON† AND F. G. LEPPINGTON
Department of Mathematics, Imperial College, London

(Received 13 July 1973)

The interaction between an acoustic source, an unstable shear layer and a large inhomogeneous solid surface is studied, using an idealized model in which a vortex sheet is generated by uniform subsonic flow on one side of a semi-infinite plate, and subjected to line-source irradiation. Both the steady-state (time-harmonic) and initial-value (impulsive source) situations are examined. In particular, the time-harmonic field which can develop in a causal manner from a quiescent initial state is examined, and a specific criterion is given by which one may obtain the correct causal harmonic solution without explicit consideration of an initial-value problem. The satisfaction of this criterion demands not only the presence in the harmonic problem of the Helmholtz instability of an infinite vortex sheet (Jones & Morgan 1972), but additionally the presence of an *edge-scatttered instability* which in real time consists of a singular line plus a tail. The harmonic solution is discussed in some detail, and the consequences of omitting the unstable solutions and thereby violating causality are shown greatly to affect the diffracted field in some circumstances. The general features of the initial-value problem are also dealt with, the various waves being classified and their arrival times at any point being given in simple form. The paper ends with some speculations as to the applicability of these phenomena to the description of the process of 'parametric amplification', by which sound generated within a duct can be greatly amplified in the far field by triggering unstable modes on the shear layer shed from the duct.

## 1. Introduction

This investigation concerns the problem of a vortex sheet behind a semi-infinite plate, separating an ambient fluid from a stream moving with uniform speed $U$. The plane occupies the region $x < 0$, $y = 0$ in a Cartesian co-ordinate system and the vortex sheet has the undisturbed position $x > 0$, $y = 0$, with moving fluid in $y < 0$ and still fluid in the half-space $y > 0$. This steady flow is considered to be disturbed by a line source in the ambient fluid ($y > 0$), and the model is intended to represent the interaction between the scattering edge and the instability waves that are triggered by such a disturbance.

A natural simplification of the problem is obtained by considering the disturbance to be simple harmonic in time $t$ with frequency $\omega$, whence

† Present address: Engineering Department, University of Cambridge.

the time dependence is described by the factor $\exp(-i\omega t)$. The solution to the initial-value problem can then be obtained, in principle, by superposition of such harmonic solutions using the usual Fourier integral synthesis. Related work by Jones & Morgan (1972) has shown that some caution is required in specifying the harmonic time problem if the physical condition of causality is to be ensured on performing the Fourier inversion integral. These authors have shown the necessity to add on eigensolutions, that have exponentially large fields as $x \to \pm\infty$, to achieve causality.

It is a major aim of this paper to propose a simple criterion for determining the correct harmonic solution, without the need to refer explicitly to the initial-value problem. Our proposal is to solve the harmonic problem as if the frequency $\omega$ were *imaginary*, and then obtain the solution for real $\omega$ by analytic continuation with respect to $\omega$.

The impulsive line source is at the fixed position $(x_0, y_0)$ in the still fluid ($y_0 > 0$) and is of strength $\delta(t)$, where $\delta$ denotes the Dirac delta function. The potential $p(\mathbf{x}; t)$ of the disturbance is labelled with a superscript (1) or (2) according as $\mathbf{x}$ is in the still fluid ($y > 0$) or in the moving fluid ($y < 0$).

This initial-value problem then requires the solution of the field equations

$$\left(\nabla^2 - \frac{1}{a_0^2}\frac{\partial^2}{\partial t^2}\right) p^{(1)} = \delta(x - x_0)\,\delta(y - y_0)\,\delta(t) \quad (y > 0), \tag{1.1}$$

$$\left\{\nabla^2 - \frac{1}{a_0^2}\left(\frac{\partial}{\partial t} + U\frac{\partial}{\partial x}\right)^2\right\} p^{(2)} = 0 \quad (y < 0), \tag{1.2}$$

where $a_0$ denotes the sound speed in the fluid. Across the vortex sheet the linearized kinematic conditions relating the displacement $\eta(x, t)$ to the particle velocities imply that

$$\left.\begin{aligned} \left(\frac{\partial}{\partial t} + U\frac{\partial}{\partial x}\right)\eta &= \frac{\partial p^{(2)}}{\partial y} \\ \partial\eta/\partial t &= \partial p^{(1)}/\partial y \end{aligned}\right\} \quad (y = 0,\ x > 0), \tag{1.3}$$

and continuity of pressure requires

$$\left(\frac{\partial}{\partial t} + U\frac{\partial}{\partial x}\right) p^{(2)} = \frac{\partial p^{(1)}}{\partial t} \quad (y = 0,\ x > 0). \tag{1.4}$$

On the rigid half-plane, we have zero normal velocity, so that

$$\partial p^{(1)}/\partial y = \partial p^{(2)}/\partial y = 0 \quad (y = 0,\ x < 0). \tag{1.5}$$

In addition we have a causality condition $p \equiv 0$ for $t < 0$, since there is no field before the source is activated.

Finally, we need conditions to limit the singularities at the edge $(0, 0)$. These constitute a very important issue which is far from being satisfactorily resolved, and therefore worthy of some discussion here. In the absence of mean flow, i.e. for the Sommerfeld problem, a solution exists with $p = O(r^{\frac{1}{2}})$ as $r \to 0$, and to this solution may be added any eigensolution of the problem. The eigensolutions, however, are all more singular than this, and it is therefore plausible to choose the solution with $p = O(r^{\frac{1}{2}})$. A better reason for taking this solution is obtained

by considering either the half-plane problem with viscosity included (Alblas 1957) or the problem with a plate of small but finite thickness (Crighton & Leppington 1973). In either case, the Sommerfeld solution with $p = O(r^{\frac{1}{2}})$ is found to be the only one capable of matching an 'inner' solution in which the effect of viscosity or of smooth edge geometry, respectively, is properly taken into account. Alternatively, one can, as is normally done in electromagnetic diffraction theory, devise edge conditions to ensure uniqueness solely with reference to the 'outer' problem, though this procedure is not nearly as convincing in the fluid-mechanical case, where the wave equation does not uniformly approximate the full equations of motion right up to the edge.

Consider next the Sommerfeld half-plane problem with the same uniform subsonic flow on both sides of the plate. There is a particular solution of Sommerfeld's type with $p = O(r^{\frac{1}{2}})$, and there are again eigensolutions continuous everywhere except at the edge, where they are singular, and which may again be rejected. There are also eigensolutions $p_E$ discontinuous across the continuation of the half-plane (though such that the associated pressure and normal velocity are continuous there), and with $p_E = O(r^{\frac{1}{2}})$ (Jones 1972). The arbitrary coefficient in $p_E$ is a measure of the strength of the unsteady vortex sheet in the extension of the half-plane. If the edge is a leading edge then obviously the potential must be continuous across the extension, and then $p_E \equiv 0$ and $p = O(r^{\frac{1}{2}})$. Note, however, that the leading-edge velocity is *not* finite. If, on the other hand, the edge is a trailing edge, we have three possible situations: (*a*) there is no vortex sheet behind the plate, $p_E = 0$ and $p = O(r^{\frac{1}{2}})$; (*b*) there is a vortex sheet behind the plate, but we do *not* impose any Kutta condition that the edge velocity be finite, in which case $p + p_E = O(r^{\frac{1}{2}})$, $p_E$ is determined only up to a multiplicative constant and there are infinitely many solutions; (*c*) the strength of the vortex sheet is such that the velocities at the edge are finite (and in fact zero), in which case there is a unique choice of $p_E$, and this leads to $p + p_E = O(r^{\frac{3}{2}})$ (plus regular terms). One is, of course, inclined to choose (*c*), though there is as yet no 'inner' problem solved to which any outer solution could be matched, and consideration of the outer problem alone cannot lead to any preference ((*a*), (*b*) and (*c*) all lead to integrable energy density, vanishing energy flux out of the edge, etc.).

Much the same situation arises in our problem. We shall determine a solution (2.44) such that the *full Kutta condition*

$$p^{(1)} = O(r^{\frac{5}{2}}), \quad p^{(2)} = O(r^{\frac{3}{2}}) \tag{1.6}$$

(apart from regular terms) applies to the perturbation potentials. We find also, however, that eigensolutions exist with

$$p_E^{(1)} = O(r^{\frac{3}{2}}), \quad p_E^{(2)} = O(r^{\frac{1}{2}}) \quad \text{[cf. (2.50)]}, \tag{1.7}$$

these corresponding to the Sommerfeld type of solution and leading to mildly infinite velocities at the edge in the moving stream. These eigensolutions cannot be excluded by any condition relating to the energy at the edge. Moreover, they are causal. However, in the solution satisfying the full Kutta condition (1.6) there is already an *unsteady* vortex sheet behind the plate, and to change that

vortex sheet strength by an arbitrary amount while simultaneously introducing infinite edge velocities seems unreasonable. We therefore insist on (1.6), while admitting the need for a convincing demonstration of its validity.

Section 2 deals with the formal solution of the problem (1.1)–(1.6) when the potential has time dependence $\exp(-i\omega t)$, hence the wavenumber $k = \omega/a_0$. The mathematical problem thus posed for $p(\mathbf{x}; k)$ has $k$ real, but it is convenient to consider $k$ to be complex, and in particular $k$ is taken to be nearly purely imaginary. Analytic continuation, with respect to $k$, then gives the solution for real $k$. The formal integral solution for $p(\mathbf{x}; k)$ is manipulated in § 3 in order to derive asymptotics as $|k|\, r \to \infty$. Finally, it is verified in § 4 that the real-time solution $p(\mathbf{x}; t)$ obtained by Fourier inversion of the time-harmonic solution $p(\mathbf{x}; k)$ is causal. An argument is given to support the proposal that causality will be ensured, in this and similar problems, by the device of considering imaginary $k$ and obtaining the real-$k$ solution by continuation.

An appendix contains some details of the Wiener–Hopf factorization of a kernel arising in the formal solution of § 2.

## 2. Time-harmonic solution

Detailed consideration is given, first, to the case in which the potential field $p$ is simple harmonic in time, with frequency $\omega = ka_0$. The solution for general time dependence is then obtained by superposition as

$$p^{(1),(2)}(x, y; t) = \frac{1}{2\pi}\int_{-\infty}^{\infty} \phi^{(1),(2)}(x, y; k)\, e^{-ika_0 t}\, d(ka_0), \tag{2.1}$$

where

$$\phi^{(1),(2)}(x, y; k) = \int_{-\infty}^{\infty} p^{(1),(2)}(x, y; t)\, e^{ika_0 t}\, dt, \tag{2.2}$$

by Fourier synthesis. The superscripts (1) and (2) again refer to the respective regions $y > 0$ and $y < 0$.

It is mathematically convenient to consider the parameter $k$ to be complex, with positive imaginary part, and the solution (2.1) is interpreted as the limit as $k_2 \to 0+$ of the integral along the path $k_1 + ik_2$, $-\infty < k_1 < \infty$.

The incident field, in the still fluid $y > 0$, is now subtracted off by writing

$$\phi^{(1)} = V + \phi, \quad \phi^{(2)} = \psi, \tag{2.3), (2.4}$$

where the line-source potential $V(x, y; k)$ is the solution for an unbounded stagnant fluid, and is given by the Hankel function

$$V = (1/4i)\, H_0^{(1)}\{k[(x - x_0)^2 + (y - y_0)^2]^{\frac{1}{2}}\}. \tag{2.5}$$

The boundary-value problem for the potentials $\phi$ and $\psi$, each proportional to $\exp(-ika_0 t)$, is found from (1.1)–(1.6) to be

$$(\nabla^2 + k^2)\,\phi = 0, \tag{2.6}$$

$$[\nabla^2 - (M\,\partial/\partial x - ik)^2]\,\psi = 0, \tag{2.7}$$

$$\left.\begin{aligned} &-i\omega\eta + U\,\partial\eta/\partial x = \partial\psi/\partial y \\ &-i\omega\eta = \partial V/\partial y + \partial\phi/\partial y \\ &-i\omega\psi + U\,\partial\psi/\partial x = -i\omega V - i\omega\phi \end{aligned}\right\} \quad (y = 0,\ x > 0), \tag{2.8}$$

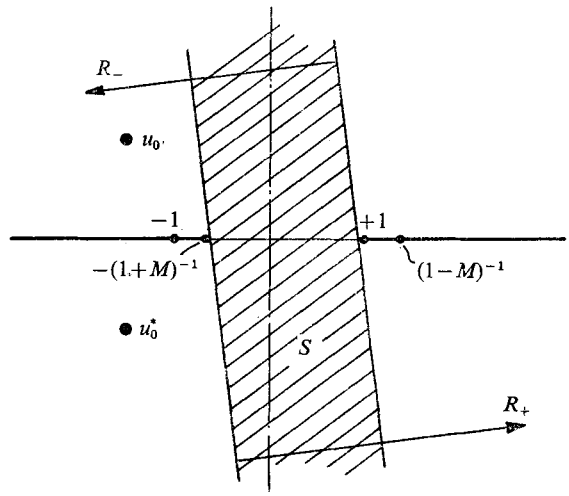


FIGURE 1. The complex-$s$ plane, with branch cuts from $s = -1$ and $s = -(1+M)^{-1}$ to $-\infty$ and from $s = +1$ and $+(1-M)^{-1}$ to $+\infty$. Also shown are the Helmholtz instability wavenumbers $u_0$ and $u_0^*$, the domains $R_\pm$ of analyticity of plus and minus functions, and the strip $S$ of overlap.

$$\partial\psi/\partial y = 0, \quad \partial\phi/\partial y = -\partial V/\partial y \quad (y = 0, x < 0), \tag{2.9}$$

with the full Kutta regularity conditions

$$V + \phi = O(r^{\frac{1}{2}}), \quad \psi - \psi_0 = O(r^{\frac{3}{2}}), \quad \eta = O(x^{\frac{3}{2}}) \tag{2.10}$$

at the edge. $M$ is the Mach number $U/a_0$, assumed less than unity.

We look for a solution that is analytic in $k$, for $k_2 > 0$. To do this, it is convenient to solve the problem (2.6)–(2.10) when the argument of $k$ is close to $\frac{1}{2}\pi$ (the precise bounds on arg $k$ are given by (2.34)). The solution for $0 < \arg k < \pi$ will then be deduced by analytic continuation.

The boundary condition at infinity, required to complete the specifications of the problem, is that $\phi$ and $\psi$ are exponentially small as $r = (x^2+y^2)^{\frac{1}{2}} \to \infty$. It will be shown later that the analytic continuation of $\phi$ (and $\psi$), to values of $|\arg k - \frac{1}{2}\pi|$ that exceed a certain critical value (dependent on the Mach number $M$), inevitably involves a field that *increases* exponentially with $r$, for some values of the polar angle $\theta$. The significance of this property will be discussed later, but for the moment our attention is confined to the case in which $k$ is nearly imaginary.

To analyse the problem (2.6)–(2.10), define the half-range Fourier transforms

$$\Phi_\pm(s, y) = \int_{-\infty}^{\infty} \phi(x, y)\, H(\pm x) \exp(iksx)\, dx, \tag{2.11}$$

and similarly for the transforms $\Psi$ and $Z$ of $\psi$ and $\eta$, where $H$ denotes the Heaviside unit function. We seek the radiating acoustic solutions that decay like $\exp(-k_2|x|)$ or $\exp[-k_2|x|/(1 \pm M)]$ as $x \to \pm\infty$. Thus all 'plus' functions, denoted by a subscript $+$, will be analytic for $s$ in the region

$$R_+: \quad \mathrm{Im}(ks) > -(1+M)^{-1} \mathrm{Im}\, k, \tag{2.12}$$

whilst all 'minus' functions, denoted by the subscript $-$, are analytic in

$$R_-: \quad \mathrm{Im}\,(ks) < \mathrm{Im}\,k. \tag{2.13}$$

There is evidently a strip

$$S: \quad -(1+M)^{-1}\,\mathrm{Im}\,k < \mathrm{Im}\,(ks) < \mathrm{Im}\,k \tag{2.14}$$

in which the full-range Fourier transforms

$$\Phi = \Phi_+ + \Phi_- = \int_{-\infty}^{\infty} \phi(x,y)\exp(iksx)\,dx, \tag{2.15}$$

and similarly $\Psi$ and $Z$, are analytic functions of $s$ (see figure 1).

The 'plus' region $R_+$ contains the real axis from $s = -(1+M)^{-1}$ to $\infty$, and $R_-$ contains the real axis from $-\infty$ to $+1$.

We now introduce the square-root functions

$$\gamma_s = (s^2-1)^{\frac{1}{2}}, \quad \varpi_s = \{s^2-(1+Ms)^2\}^{\frac{1}{2}}, \tag{2.16), (2.17}$$

where $\gamma_s$ has cuts from $\pm 1$ to $\pm\infty$, and $\varpi_s$ has cuts from $\pm(1\mp M)^{-1}$ to $\pm\infty$. Each of the functions is chosen to be positive when $s$ is large and just below the positive real axis. With these definitions, it is found that $\mathrm{Re}\,(k\gamma_s) > 0$ and $\mathrm{Re}\,(k\varpi_s) > 0$ throughout the strip $S$.

The transform of the incident potential $V(x,y)$ of formula (2.5) may be evaluated as

$$V(s,y) = -(2k\gamma_s)^{-1}\exp\{iksx_0 - k\gamma_s|y-y_0|\}, \tag{2.18}$$

and the transformed field equations (2.6) and (2.7) take the form

$$(d^2/dy^2 - k^2\gamma_s^2)\,\Phi = 0 \tag{2.19}$$

and

$$(d^2/dy^2 - k^2\varpi_s^2)\,\Psi = 0. \tag{2.20}$$

Since $\Phi$ and $\Psi$ must vanish as $|y| \to \infty$, for $s$ in the strip $S$, we have

$$\Phi(s,y) = \Phi(s,0)\exp(-k\gamma_s y) \tag{2.21}$$

and

$$\Psi(s,y) = \Psi(s,0)\exp(+k\varpi_s y), \tag{2.22}$$

from which it follows that

$$\Phi'_+ + \Phi'_- = -k\gamma_s(\Phi_+ + \Phi_-) \tag{2.23}$$

and

$$\Psi'_+ + \Psi'_- = +k\varpi_s(\Psi_+ + \Psi_-). \tag{2.24}$$

The prime denotes $d/dy$, while here and henceforth all the functions are evaluated at $y = 0$ unless explicitly stated otherwise.

The boundary conditions (2.8)–(2.10) become

$$\left.\begin{aligned} -i\omega D_s Z_+ = \Psi'_+, \quad -i\omega Z_+ = V'_+ + \Phi'_+, \\ -i\omega D_s \Psi_+ = -i\omega V_+ - i\omega\Phi_+ + U\psi_0, \end{aligned}\right\} \tag{2.25}$$

$$\Psi'_- = 0, \quad \Phi'_- = -V'_-, \tag{2.26}$$

$$\Phi_- = O(s^{-1}), \quad \Psi_- = \psi_0/(iks) + O(s^{-\frac{3}{2}}), \quad Z_+ = O(s^{-\frac{3}{2}}) \quad \text{as} \quad |s| \to \infty, \tag{2.27}$$

where

$$D_s = 1 + Ms, \tag{2.28}$$

$\psi_0$ denotes $\psi(0,0)$ and use has been made of the constraint $\eta(0) = 0$.

Elimination of all the unknown 'plus' functions except $Z_+$ leads to the equation

$$-i(\omega/k)\,K(s)\,Z_+ = D_s\Psi'_- - \Phi_- + i(U/\omega)\,\psi_0 + (k\gamma_s)^{-1}\,V' + V_+, \tag{2.29}$$

where

$$K(s) = \gamma_s^{-1} + D_s^2/\varpi_s. \tag{2.30}$$

Now according to (2.18),

$$V'(s,0) = k\gamma_s\,V(s,0),$$

so that

$$(k\gamma_s)^{-1}\,V' + V_+ = 2V - V_-,$$

and (2.29) may be expressed in the form of a Wiener–Hopf equation:

$$-i(\omega/k)\,KZ_+ = F_- + 2V, \tag{2.31}$$

where

$$F_- = D\Psi'_- - \Phi_- + iU\psi_0/\omega - V_-.$$

It is shown in the appendix that the Wiener–Hopf kernel function $K(s)$, given by (2.30), has its zeros at the complex conjugate points $u_0$ and $u_0^*$, given by

$$u_0 = -u_1 + iu_2 = -\cos(\tfrac{1}{4}\pi + i\tau_0), \tag{2.32}$$

where $\tau_0$ is the positive root of the equation

$$\cosh\tau_0 = 2^{-\frac{1}{2}}M^{-1}\{1 + (1+M^2)^{\frac{1}{2}}\}. \tag{2.33}$$

In particular, the kernel $K$ has no zeros in the strip $S$, provided that the argument of $k$ is sufficiently close to $\frac{1}{2}\pi$. To be precise, if

$$|\arg k - \tfrac{1}{2}\pi| < \tan^{-1}\{[u_1 - (1+M)^{-1}]/u_2\}, \tag{2.34}$$

with $u_1$ and $u_2$ defined by (2.32).

The standard Wiener–Hopf procedure (Noble 1958, chap. 1, § 7) requires a factorization of the kernel $K(s)$ as a product $K_+(s)\,K_-(s)$ of functions that are analytic and non-zero in the respective regions $R_+$ and $R_-$. If we write

$$K(s) = (s-u_0)\,(s-u_0^*)\,\kappa(s),$$

the function $\kappa(s)$ has no zeros in the cut $s$ plane, and has the factorization

$$\kappa(s) = \kappa_+(s)\,\kappa_-(s)$$

that is described in the appendix, with $\kappa_\pm(s)$ of order $s^{-\frac{1}{2}}$ as $|s| \to \infty$. It follows that the required functions $K_\pm(s)$ are given by

$$\left.\begin{aligned} K_+(s) &= (s-u_0)\,(s-u_0^*)\,\kappa_+(s) \\ \text{and} \qquad K_-(s) &= \kappa_-(s), \end{aligned}\right\} \tag{2.35}$$

with

$$K_+ = O(s^{\frac{3}{2}}), \quad K_- = O(s^{-\frac{1}{2}}) \quad \text{as} \quad |s| \to \infty \tag{2.36}$$

in the respective regions $R_+$ and $R_-$.

On dividing (2.31) by $K_-(s)$, and decomposing the function

$$2V/K_- \equiv P(s) = P_+ + P_- \tag{2.37}$$

into a sum of 'plus' and 'minus' functions, we get

$$-i(\omega/k)\,K_+Z_+ - P_+ = F_-/K_- + P_- \equiv E(s). \tag{2.38}$$

At this stage, (2.38) is valid only within the strip $S$, but since the left and right sides are valid in the respective regions $R_+$ and $R_-$, they provide analytic continuations of each other and together define a function $E(s)$ that is analytic in the whole complex-$s$ plane. Further, the regularity conditions (2.27), together with the bounds (2.36) and the evident smallness at infinity of $P_\pm(s)$ and $V_\pm(s)$, imply that each side of formula (2.38) tends to zero as $|s| \to \infty$. According to Liouville's theorem, the analytic function $E(s)$ must therefore be zero. In particular,

$$-i(\omega/k)\,Z_+ = P_+/K_+ \tag{2.39}$$

and the scattered potential transform $\Phi$ in the ambient fluid $y > 0$ is therefore given by formulae (2.23)–(2.26) and (2.18) as

$$\Phi = V + i\omega(k\gamma_s)^{-1} Z_+,$$

whence

$$\Phi(s,y) = \{V - (\gamma_s K_+)^{-1} P_+\} \exp(-k\gamma_s y), \tag{2.40}$$

from (2.21) and (2.39).

Inversion of the first term gives a contribution

$$\phi_r = -\frac{1}{2\pi}\int_\Gamma (2k\gamma_s)^{-1} \exp\{iks(x_0 - x) - k\gamma_s(y + y_0)\}\, d(ks) \tag{2.41}$$

evaluated along the straight-line contour $\Gamma$ in the strip $S$:

$$\Gamma: \quad s = p\,e^{-i\alpha}, \quad -\infty < p < \infty, \quad \alpha = \arg k. \tag{2.42}$$

The integral (2.41) is recognized as a Hankel function, so

$$\phi_r = (4i)^{-1} H_0^{(1)}\{k[(x - x_0)^2 + (y + y_0)^2]^{\frac{1}{2}}\} \tag{2.43}$$

and represents the reflected field, as if the rigid plate occupied the whole plane $y = 0$.

Inversion of the second term of (2.40) gives

$$\phi - \phi_r = -(2\pi)^{-1} \int_\Gamma \exp\{-iksx - k\gamma_s y\} \frac{P_+(s)}{\gamma_s K_+(s)}\, d(ks).$$

Now the usual Cauchy integral expression for the 'plus' function $P_+$, defined by (2.37), is

$$P_+(s) = \frac{1}{2\pi i}\int_{\Gamma'} \frac{P(t)}{t - s}\, dt, \quad s \in \Gamma,$$

$$= -\frac{1}{2\pi i}\int_{\Gamma'} \frac{\exp\{iktx_0 - k\gamma_t y_0\}}{k\gamma_t K_-(t)} \frac{dt}{t - s},$$

where $\Gamma'$ lies just to the left of $\Gamma$, but remains in the strip $S$.

Thus the field, for $y > 0$, is given by

$$\phi = \phi_r + \frac{1}{4\pi^2 i}\int_\Gamma ds \int_{\Gamma'} \frac{\exp\{-iksx - k\gamma_s y + iktx_0 - k\gamma_t y_0\}\, dt}{\gamma_s \gamma_t (s - u_0)(s - u_0^*)\, \kappa_+(s)\, \kappa_-(t)\, (t - s)}, \tag{2.44}$$

with $\Gamma$ and $\Gamma'$ shown in figure 2. Note that the integrand depends on $k$ only where explicitly shown, in the exponent; the paths of integration also depend on $k$, being at an angle $-\arg k$ to the real axis.

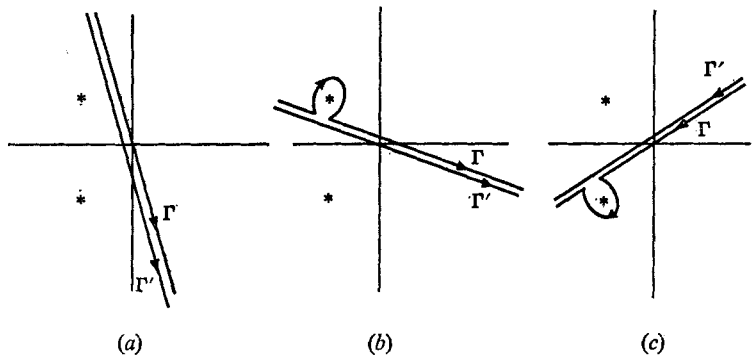


FIGURE 2. Contours $\Gamma$ and $\Gamma'$ in the $s$ plane defining $\phi$ through (2.44) as an analytic function of $k$ when Im $k > 0$ and (*a*) $|\arg k - \frac{1}{2}\pi| < \tan^{-1}(u_1/u_2)$, (*b*) $\arg k < \frac{1}{2}\pi - \tan^{-1}(u_1/u_2)$, (*c*) $\arg k > \frac{1}{2}\pi + \tan^{-1}(u_1/u_2)$.

At this stage we have insisted that $\arg k$ be sufficiently close to $\frac{1}{2}\pi$ to ensure that the contours $\Gamma$ and $\Gamma'$ are well away from the singular points $u_0$ and $u_0^*$. We now define $\phi$, for all values of $\arg k$ in the range $0 < \arg k < \pi$, by simply taking the analytic continuation of formula (2.44). Thus when $|\arg k - \frac{1}{2}\pi|$ increases, so that $\Gamma$ and $\Gamma'$ approach $u_0$ or $u_0^*$, the contour $\Gamma$ has to be deformed so as not to cross these poles (figure 2). There is no pole at $t = u_0, u_0^*$ and therefore no need to indent the path $\Gamma'$.

The field in the moving fluid, $y < 0$, is found from formulae (2.24)–(2.26) and (2.39) to be

$$\Psi = (k\varpi_s)^{-1} i\omega D_s Z_+ = -(D_s/\varpi_s)(P_+/K_+), \tag{2.45}$$

thus

$$\psi = \frac{1}{4\pi^2 i}\int_\Gamma ds \int_{\Gamma'} \frac{D_s \exp\{-iksx + k\varpi_s y + iktx_0 - k\gamma_t y_0\}\, dt}{\varpi_s \gamma_t (s-u_0)(s-u_0^*)\kappa_+(s)\kappa_-(t)(t-s)}, \tag{2.46}$$

along the contours $\Gamma$ and $\Gamma'$ of figure 2.

Finally, it is instructive to examine the relationship between the solution (2.44) for $\phi$ and that which would have been obtained from the more conventional procedure of taking $k$ to be nearly real from the outset. To be definite, take $k = k_1 + ik_2$, with $k_1$ and $k_2$ positive and $k_2$ very small. The Wiener–Hopf analysis goes through almost as before, but with the crucial difference that the zero $s = u_0$ of the kernel $K(s)$ now lies in the 'plus' region $R_+$. This implies that the correct factorization $K = \hat{K}_+ \hat{K}_-$ is then given by

$$\hat{K}_+ = (s-u_0^*)\kappa_+, \quad \hat{K}_- = (s-u_0)\kappa_- \tag{2.47}$$

in place of (2.35), and formula (2.38) has $K_\pm$ and $E$ replaced by $\hat{K}_\pm$ and $\hat{E}$. The analytic function $\hat{E}$ is again zero, but since $\hat{K}_\pm$ are now of order $s^{\frac{1}{2}}$ at $\infty$, this ensures only that $Z_+$ is of order $s^{-\frac{3}{2}}$ as $|s| \to \infty$, whence $\eta = O(x^{\frac{1}{2}})$ and $\psi - \psi_0 = O(x^{\frac{1}{2}})$ as $x \to 0$. One finds, in fact, that the coefficients implied by the $O$-symbols are non-zero, and hence that the fields *do not satisfy the edge requirement* (2.10); evidently an eigensolution of the problem (which must necessarily be large as $x \to \pm\infty$) must be added to remedy this defect.

The bounded solution $\hat{\phi}$, when $k$ is nearly real, is given by a formula analogous to (2.44), viz.

$$\hat{\phi} = \phi_r + \frac{1}{4\pi^2 i}\int_{\hat{\Gamma}} ds \int_{\hat{\Gamma}'} \frac{\exp(-iksx - k\gamma_s y + iktx_0 - k\gamma_t y_0)}{\gamma_s \gamma_t (s-u_0^*)\,\kappa_+(s)\,(t-u_0)\,\kappa_-(t)} \frac{dt}{t-s}, \tag{2.48}$$

where the contours $\hat{\Gamma}$ and $\hat{\Gamma}'$ are inclined at an angle $-\arg k$ to the real axis, and are similar to those of figure 2(*b*), but with *no deformation* round the pole $s = u_0$.

The difference between the two solutions $\phi$ and $\hat{\phi}$ is given from (2.44) and (2.48) as

$$\begin{aligned}\phi - \hat{\phi} = &-\frac{1}{2\pi}\frac{\exp(-iku_0 x - k\gamma_0 y)}{\gamma_0(u_0-u_0^*)\,\kappa_+(u_0)}\int_{\hat{\Gamma}'} \frac{\exp(iktx_0 - k\gamma_t y_0)}{\gamma_t \kappa_-(t)\,(t-u_0)}\,dt \\ &+\frac{1}{4\pi^2 i}\int_{\hat{\Gamma}} \frac{\exp(-iksx - k\gamma_s y)}{\gamma_s (s-u_0)\,(s-u_0^*)\,\kappa_+(s)}\,ds \int_{\hat{\Gamma}'} \frac{\exp(iktx_0 - k\gamma_t y_0)}{\gamma_t \kappa_-(t)\,(t-u_0)}\,dt,\end{aligned} \tag{2.49}$$

where $\gamma_0 = u_2 - iu_1$ is the value of $\gamma_s$ when $s = u_0$. The first term arises from the pole contribution to $\phi$ at $s = u_0$, and the double integral accounts for the difference in the integrands in formulae (2.44) and (2.48). We see that the difference $\phi - \hat{\phi}$ is just a multiple of the eigensolution

$$\phi_E = \exp(-iku_0 x - k\gamma_0 y) - \frac{1}{2\pi i}\int_{\hat{\Gamma}} \frac{\exp(-iksx - k\gamma_s y)\,ds}{\gamma_s (s-u_0)\,(s-u_0^*)\,\kappa_+(s)}\,\gamma_0 (u-u_0^*)\,\kappa_+(u_0) \tag{2.50}$$

that has been derived earlier by Crighton (1972*a*). It is easy to verify that $\phi_E$ does not satisfy the required edge condition (2.10) (with $V$ replaced by zero) and that the multiple of $\phi_E$ which must be added to $\hat{\phi}$ to give the correct edge condition is precisely the one indicated above, and finally yields our original solution $\phi$ of formula (2.44).

The fact that the eigensolution $\phi_E$ is unbounded, as $x \to \infty$, might seem to indicate that the solution $\hat{\phi}$ is preferable to $\phi$, since it apparently sacrifices the edge condition in favour of the more desirable condition of boundedness at infinity. But this is illusory, since it can easily be shown that the analytic continuation of $\hat{\phi}$ with respect to $k$ will inevitably produce terms that are large at infinity, for some values of $k$: such terms arise when $\arg k$ increases beyond $\tan^{-1}(u_2/u_1)$ and $\pi - \tan^{-1}(u_2/u_1)$, when the contour $\hat{\Gamma}$ crosses the poles $u_0$ and $u_0^*$. Thus if $\phi$ is to be analytic with respect to $k$, then it *must be unbounded at* $\infty$ *for some values of* $\arg k$, and there is nothing to be gained by relaxing the edge conditions (2.10).

The real-time solution of our initial-value problem (1.1)–(1.6) requires an interpretation of the inversion integral (2.1). This is a far from trivial matter, in view of the exponentially large terms that are inherent in our solution, for some values of $k$, and we shall return to this matter in § 4. To pave the way for this analysis the next section concerns the manipulation of the double integral (2.44), in order to estimate the behaviour of our solution for large values of $|k|\,r$.

## 3. Solution for large $kr$

Polar co-ordinates $(r, \theta)$ and $(r_0, \theta_0)$ are defined by the usual formulae:

$$x = r\cos\theta, \quad y = r\sin\theta; \quad x_0 = r_0\cos\theta_0, \quad y = r_0\sin\theta. \tag{3.1}$$

To limit the number of possibilities $\theta_0$ is restricted to lie within the open region $(0, \frac{1}{2}\pi)$, and confining our attention to the potential $\phi$ in the stagnant fluid, we have $0 < \theta < \pi$. Polar co-ordinates $(r_1, \theta_1)$ based on the image point are also defined as

$$x - x_0 = r_1\cos\theta_1, \quad y + y_0 = r_1\sin\theta_1. \tag{3.2}$$

Now for any $\theta_0 \in (0, \frac{1}{2}\pi)$, the $t$ path $(\Gamma')$ of integral (2.44) may be deformed onto the hyperbolic path $t = \cos(\theta_0 + i\lambda)$, where $\lambda$ is real and runs from $-\infty$ to $+\infty$, without crossing any branch line, and with no contributions from the linking arcs at infinity. The value of $\gamma_t$ is $-i\sin(\theta_0 + i\lambda)$, and then

$$\exp(iktx_0 - k\gamma_t y_0) = \exp(ikr_0\cosh\lambda). \tag{3.3}$$

For the moment we ignore possible pole contributions from this, and from the next move, which is to deform the $s$ path $(\Gamma)$ of (2.44) onto a branch of the hyperbola $s = -\cos(\theta + i\tau)$, $-\tau < \infty < \tau$. The appropriate branch of the hyperbola is in the left or right half-plane according as $\theta < \frac{1}{2}\pi$ or $\theta > \frac{1}{2}\pi$. In neither case is there any contribution from the linking arcs at infinity.

There is no difficulty with branch cuts, except if $\theta$ is sufficiently close to 0. Define a Mach angle by

$$\cos\theta_M = (1+M)^{-1}, \quad 0 < \theta_M < \tfrac{1}{2}\pi. \tag{3.4}$$

Then if $0 < \theta < \theta_M$ the hyperbolic $s$ path cuts the branch line from $s = -(1+M)^{-1}$, and it will be necessary to add, to the integral over the hyperbolic path, an additional integral round the branch cut from $s = -\cos\theta + 0i$ to $s = -\cos\theta - 0i$ via the branch point $s = -\cos\theta_M$. This extra field, which makes a smaller contribution than the reflected and transmitted fields, is the *secondary bow wave* field, heard for $\theta < \theta_M$, and arises because the moving fluid causes a disturbance to propagate along the boundary of the stagnant fluid at the supersonic speed $U + a_0$. For the present the bow wave field will be ignored, supposing that $\theta_M < \theta < \pi$.

Thus on leaving aside all pole contributions that may arise from the deformations described above, we are left with a double $(\tau, \lambda)$ integral which we identify as the diffracted wave:

$$\phi_d = \frac{1}{4\pi^2 i}\int_{-\infty}^{\infty} d\tau \int_{-\infty}^{\infty} d\lambda \; \frac{\exp(ikr\cosh\tau + ikr_0\cosh\lambda)}{\{\cos(\theta+i\tau)+u_0\}\{\cos(\theta+i\tau)+u_0^*\}\kappa_+\{-\cos(\theta+i\tau)\} \times \kappa_-\{\cos(\theta_0+i\lambda)\}\{\cos(\theta+i\tau)+\cos(\theta_0+i\lambda)\}}. \tag{3.5}$$

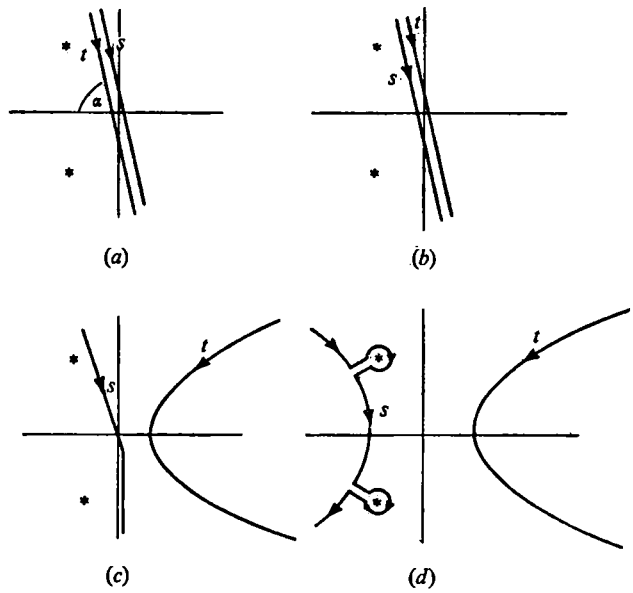


FIGURE 3. Showing the $t$ and $s$ paths when $k$ is nearly imaginary, as in figure 2($a$). If $\alpha$ is close to 0 or $\pi$, then the $s$ path is indented, as in figures 2($b$) and ($c$) respectively, so as not to cross the poles at $s = u_0$ and $s = u_0^*$.

In particular, if $k$ is now taken to be real and positive, a standard stationary-phase calculation shows that, for large $kr$,

$$\phi_d \sim \frac{1}{4\pi^2 i}\left(\frac{2\pi}{kr}\right)^{\frac{1}{2}} e^{ikr+\frac{1}{4}i\pi}\frac{(\cos\theta+u_0)^{-1}(\cos\theta+u_0^*)^{-1}}{\kappa_+(-\cos\theta)} \times\int_{-\infty}^{\infty}\frac{\exp(ikr_0\cosh\lambda)\,d\lambda}{\kappa_-\{\cos(\theta_0+i\lambda)\}\{\cos\theta+\cos(\theta_0+i\lambda)\}}. \tag{3.6}$$

For small values of the Mach number $M$ we may use the estimates (A 7), (A 12) and (A 13) for $u_0$, $u_0^*$, $\kappa_+$ and $\kappa_-$. If $kr$ and $kr_0$ are both large we get

$$\phi_d \sim \frac{\exp\{i(kr+kr_0-\frac{1}{2}\pi)\}}{2\pi k(rr_0)^{\frac{1}{2}}}\frac{\sin\frac{1}{2}\theta\sin\frac{1}{2}\theta_0}{\cos\theta+\cos\theta_0}, \tag{3.7}$$

which reproduces the Sommerfeld solution for scattering with no flow. Similarly, if $kr \gg 1$ and $kr_0 \ll 1$ we have

$$\phi_d \sim \pi^{-1}(r_0/r)^{\frac{1}{2}}\sin\tfrac{1}{2}\theta\sin\tfrac{1}{2}\theta_0\exp(ikr+\tfrac{1}{4}\pi i), \tag{3.8}$$

which is again the Sommerfeld result for no flow.

It is of interest to compare these results with those for the potential $\hat{\phi}$ that would be obtained by taking real $k$ and neglecting to add the eigensolution $\phi_E$ to ensure causality. The difference $\phi-\hat{\phi}$, given by formula (2.49), can be manipulated in the manner described above, whence it is found that

$$\phi-\hat{\phi} = O(M)\times\text{Sommerfeld solution}, \quad kr \gg 1, \quad kr_0 \gg 1,$$

so that the error is insignificant for small $M$. But if the field point is sufficiently close to the edge, specifically if $kr_0 \ll M$, then

$$\phi - \hat{\phi} \sim \pi^{-1}(r_0/r)^{\frac{1}{2}} \sin \tfrac{1}{2}\theta \sin \tfrac{1}{2}\theta_0 \exp(ikr + \tfrac{1}{4}\pi i), \tag{3.9}$$

which is precisely the same as the result (3.8) for $\phi_d$. Thus $\hat{\phi} = o(\phi_d)$ and we conclude that the potential $\hat{\phi}$ is quite incorrect for sources in the small region close to the edge. The importance of these results is discussed at greater length in § 6 below.

Next we look at the pole contributions to the integral (2.44) which arise at $t = s$ and at $s = u_0 = -u_1 + iu_2$ and $s = u_0^* = -u_1 - iu_2$, with $u_1$ and $u_2$ given by (2.32). Suppose first that

$$\theta_M < \theta < \pi - \theta_0. \tag{3.10}$$

Then we get to the hyperbolic paths, described above, by the sequence of deformations $(a) \to (b) \to (c) \to (d)$ shown in figure 3.

First, deform the $t$ path ($\Gamma'$) of integral (2.44) above the $s$ path ($\Gamma$) (figures $3a \to b$) to produce a residue field from the pole at $t = s$. When added to the reflected field $\phi_r$ this gives a contribution

$$\phi_v = \frac{1}{2\pi}\int_\Gamma \left\{-\frac{1}{2\gamma_s} + \frac{1}{\gamma_s^2 K(s)}\right\} \exp\{-iks(x-x_0) - k\gamma_s(y+y_0)\}\, ds, \tag{3.11}$$

along the path $\Gamma$, indented if necessary, of figure 2. This potential $\phi_v$ represents the field scattered by a *doubly infinite* vortex sheet and is precisely the field discussed by Jones & Morgan (1972), including their exponentially growing eigensolution, but in a different notation. To facilitate the comparison with that work, note that if $k$ is nearly real (and positive, say) then the $\Gamma$ integral of figure 2 ($b$) is deformed round the pole $s = u_0$; this pole yields the residue contribution

$$\frac{-i\exp\{-iku_0(x-x_0) - k\gamma_0(y+y_0)\}}{\gamma_0^2(u_0 - u_0^*)\kappa(u_0)}, \tag{3.12}$$

which is the exponentially growing field added by Jones & Morgan to ensure causality.

Now deform the $t$ path onto the hyperbola $t = \cos(\theta_0 + i\lambda)$, if necessary bending the $s$ path to avoid crossing the hyperbola. (For example, the deformation shown in figure 3 ($c$), from $s = \infty e^{-i\alpha}$ to $s = \infty \times e^{-\frac{1}{2}\pi i}$, achieves this aim for all $\theta < \pi - \alpha$.) No poles are crossed and there are no contributions from arcs at infinity.

Finally, deform the $s$ path onto the hyperbola $s = -\cos(\theta + i\tau)$ (figures $3c \to d$), an operation which captures both poles $u_0$ and $u_0^*$ or none, according as $\theta < \frac{1}{4}\pi$ or $\theta > \frac{1}{4}\pi$. If the residue contribution from these poles is denoted by $\phi_e$, then the potential $\phi$ in the still fluid is

$$\phi = \phi_d + \phi_v + \phi_e, \quad \theta_M < \theta < \pi - \theta_0, \tag{3.13}$$

where $\phi_d$ and $\phi_v$ are given by (3.5) and (3.11) and

$$\begin{aligned}\phi_e = &-\frac{\exp(-iku_0 x - k\gamma_0 y)}{2\pi\gamma_0(u_0 - u_0^*)\kappa_+(u_0)} \int_{-\infty}^{\infty} \frac{\exp(ikr_0\cosh\lambda)\, d\lambda}{\kappa_-\{\cos(\theta_0 + i\lambda)\}\{\cos(\theta_0 + i\lambda) - u_0\}} \\ &-\frac{\exp(-iku_0^* x - k\gamma_0^* y)}{2\pi\gamma_0^*(u_0^* - u_0)\kappa_+(u_0)} \int_{-\infty}^{\infty} \frac{\exp(ikr_0\cosh\lambda)\, d\lambda}{\kappa_-\{\cos(\theta_0 + i\lambda)\}\{\cos(\theta_0 + i\lambda) - u_0^*\}}\end{aligned} \tag{3.14}$$

for $\theta < \frac{1}{4}\pi$, with $\phi_e$ zero for $\theta > \frac{1}{4}\pi$.

If $\theta < \theta_M$ then we must add to (3.13) the secondary bow wave field

$$\phi_{2b} = \frac{1}{4\pi^2 i}\int_L \frac{\exp(-iksx - k\gamma_s y)\,ds}{\gamma_s(s-u_0)(s-u_0^*)\kappa_+(s)}\int_{-\infty}^{\infty}\frac{\exp(ikr_0\cosh\lambda)\,d\lambda}{\kappa_-(t)\{\cos(\theta_0+i\lambda)-s\}}, \tag{3.15}$$

where $L$ is the loop from $s = -\cos\theta - 0i$ to $s = -\cos\theta + 0i$ via the branch point $s = -\cos\theta_M$.

If $\pi - \theta_0 < \theta < \pi$ then the appropriate hyperbola for the $s$ path lies to the right of the hyperbola for the $t$ path. In this case we do *not* perform the operation (figures $3a \to b$) of moving $\Gamma'$ to the right of $\Gamma$. The hyperbolic paths are reached without any poles being crossed, to get

$$\phi = \phi_d + \phi_r, \quad \pi - \theta_0 < \theta < \pi, \tag{3.16}$$

with $\phi_d$ and $\phi_r$ given by (3.5) and (2.43).

In formula (3.13), the diffracted field $\phi_d$, whose integrand becomes singular at $\theta = \frac{1}{4}\pi$, plays the role of smoothing out the discontinuity of the field $\phi_e$, which cuts off abruptly at $\theta = \frac{1}{4}\pi$.

It is to be noted that the diffracted field $\phi_d$, and also the reflected field $\phi_r$, is exponentially small as $|k| \to \infty$ in the upper half-plane. This ensures a causal solution for the inversion integral corresponding to this potential. The potentials $\phi_v$ and $\phi_e$, given by (3.11) and (3.14), both vanish as $k_2 \to \infty$ with $k_1$ fixed. This is indeed ensured by our original formulation, which required $\arg k$ to be close to $\frac{1}{2}\pi$. But if $|\arg k - \frac{1}{2}\pi|$ exceeds the value $\tan^{-1}(u_1/u_2)$, on the other hand, then the waves $\exp(-iku_0 x - k\gamma_0 y)$ and $\exp(-iku_0^* x - k\gamma_0^* y)$ *increase* exponentially with $|k|$ for some values of $(x, y)$, namely when

$$(x-y)/(x+y) > |k_2/k_1|\,(u_1/u_2). \tag{3.17}$$

Equivalently, these wave modes increase exponentially as $r \to \infty$ along rays that satisfy (3.17).

This behaviour is an inevitable consequence of the Helmholtz-type instability of the basic flow, and the transform of any causal solution must have such a property. It follows that the real-time solution cannot be expressed in terms of ordinary functions for all $(x, y)$, and we follow Jones & Morgan (1972) in interpreting the solutions in terms of delta functions of complex variables (ultradistributions). It is proposed here that the criteria for a causal solution, in this and in similar problems, are that $\phi(x, y; k)$ must be *analytic in* $k$, in the upper half-plane $k_2 > 0$, and that $\phi \to 0$ *as* $k_2 \to \infty$ *with* $k_1$ *fixed*. In practice these criteria are most conveniently met by calculating the solution for imaginary $k$, using conventional transform techniques, with the solutions for other values of $k$ then inferred by analytic continuation.

## 4. The initial-value problem

We now turn to the task of interpreting the Fourier inversion formula

$$p_\alpha(x, y; t) = \frac{a_0}{2\pi}\int_{-\infty+i0}^{\infty+i0}\phi_\alpha(x, y; k)\,e^{-ika_0 t}\,dk \tag{4.1}$$

for the various fields $\phi_d$, $\phi_v$, $\phi_r$, $\phi_e$ and $\phi_{2b}$ that are described in § 3.

Now the diffracted, reflected and bow wave potentials ($\phi_d$, $\phi_r$ and $\phi_{2b}$) are analytic functions of $k$ for $k_2 > 0$, and are exponentially small as $|k|\, r \to \infty$ along any ray ($\arg k =$ constant) in this half-plane. It follows that, in each case, the integrand of (4.1) is analytic and exponentially small as $|k| \to \infty$ in the upper half-plane for all $t < 0$, a property which may be used to show that the integral vanishes when $t < 0$, by deforming the contour onto a large semi-circle $|k| =$ constant, $k_2 > 0$. More generally the potential may vanish for some positive values of $t$, provided it is sufficiently small, as $|k| \to \infty$, to ensure that the exponentially large term $\exp(-ika_0 t)$ is dominated by the exponentially small factor arising in $\phi_\alpha(x, y; k)$.

The vortex reflected field $\phi_v$ [formula (3.11)] is also analytic in $k$, for $k_2 > 0$, and vanishes as $k_2 \to \infty$ with $k_1$ fixed, but for some values of $(x, y)$ it is exponentially large as $|k| \to \infty$ along certain rays. This field has been treated by Jones & Morgan, in terms of delta functions of complex variables (ultradistributions), and is briefly discussed here in the slightly different notation of this work.

If the contour $\Gamma$ of formula (3.11) is deformed onto the hyperbola

$$s = -\cos(\theta_1 + i\tau),$$

then we have

$$\phi_v = \phi_r + \frac{1}{2\pi}\int_{-\infty}^{\infty} (\gamma K)^{-1} \exp(ikr_1 \cosh\tau)\, d\tau, \quad \theta_1 > \tfrac{1}{4}\pi, \tag{4.2}$$

where $\phi_r$ is given by (2.43), and $(r_1, \theta_1)$ are the polar co-ordinates defined by (3.2). If $\theta_1 < \frac{1}{4}\pi$, then both the poles, $s = u_0$ and $s = u_0^*$, are crossed in the deformation and we get an additional term

$$\phi_a = A \exp\{-iku_0 x_1 - k\gamma_0 y_1\} + A^* \exp\{-iku_0^* x_1 - k\gamma_0^* y_1\}, \tag{4.3}$$

where $x_1 = x - x_0$ and $y_1 = y + y_0$; $A$ and $A^*$ are complex conjugate constants with

$$A = i\{\gamma_0^2 \kappa_-(u_0)\, \kappa_+(u_0)\, (u_0 - u_0^*)\}^{-1}. \tag{4.4}$$

Now the fields given by (4.2) are exponentially small as $|k| \to \infty$, with $k_2 > 0$, and lead to causal solutions by the standard procedure described above. As for the expression (4.3), it is exponentially small as $k_2 \to \infty$, with $k_1$ fixed, provided only that

$$x_1 + y_1 > 0. \tag{4.5}$$

This condition is certainly met in the region $(0 < \theta_1 < \frac{1}{4}\pi)$ of definition of $\phi_a$. On formally inverting the transform (4.3), in terms of delta functions of complex argument, we find that

$$\begin{aligned} p_a &= (a_0/2\pi)\int_{-\infty}^{\infty} \phi_a e^{-ika_0 t}\, dk \\ &= \mathrm{Re}\{2Aa_0\, \delta(a_0 t - u_1(x_1 + y_1) + iu_2(x_1 - y_1))\}. \end{aligned} \tag{4.6}$$

On writing

$$\delta(\alpha + i\beta) = \sum_0^\infty \frac{(i\beta)^n}{n!}\, \delta^{(n)}(\alpha), \tag{4.7}$$

we see that (4.6) is non-zero only when $t = (u_1/a_0)(x_1 + y_1)$, which is positive and corresponds to a causal solution if and only if the constraint (4.5) holds. In particular then, this solution is causal in the region $(0 < \theta_1 < \frac{1}{4}\pi)$ of definition of $\phi_a$.

Note that the exponents of the terms in formula (4.3) have real parts

$$\pm k_1 u_2(x-y) - k_2 u_1(x+y),$$

that these exponents are negative, as $k_2 \to \infty$ with $k_1$ fixed, if and only if (4.5) holds, and that this is the regime in which the ultradistribution solution (4.6) can be interpreted as being causal.

Similarly, the field $\phi_e$ given by (3.14) is analytic in the upper half $k$ plane and is exponentially small as $k_2 \to \infty$ with $k_1$ fixed. This should ensure the causality of its inverse integral; but the fact that $\phi_e$ is exponentially large as $|k| \to \infty$ in some directions ($\arg k$ = constant) indicates a causal solution only within the framework of ultradistributions, not ordinary functions. Thus a formal inversion gives

$$p_e(x,y;t) = -\tfrac{1}{2}\mathrm{Re}\left\{\frac{a_0}{\gamma_0(u_0-u_0^*)\,\kappa_+(u_0)} \times \int_{-\infty}^{\infty} \frac{\delta\{a_0 t - u_1(x+y) - r_0\cosh\lambda + iu_2(x-y)\}}{\kappa_-\{\cos(\theta_0+i\lambda)\}\{\cos(\theta_0+i\lambda)-u_0\}}\,d\lambda\right\}. \quad (4.8)$$

According to (4.7), the delta function appearing in the integrand of (4.8) is non-zero only when $a_0 t = u_1(x+y) + r_0\cosh\lambda$. In particular the solution $p_e(x,y;t)$ is zero for negative $t$ provided that

$$u_1(x+y) + r_0 > 0. \quad (4.9)$$

This is precisely the condition under which the transform solution (3.14) is small as $k_2 \to \infty$, and lends support to our proposal that the correct harmonic solution (corresponding to a causal solution) is the one which is analytic for $k_2 > 0$ and is exponentially small as $k_2 \to \infty$.

In order to interpret the integral of formula (4.8), change the variable to $c \equiv \cosh\lambda$, to get

$$p_e(\mathbf{x};t) = \mathrm{Re}\int_1^{\infty} \delta\{r_0 c - a_0 t + u_1(x+y) - iu_2(x-y)\}\,F(c)\,dc, \quad (4.10)$$

where

$$F(c) = (c^2-1)^{-\frac{1}{2}}\{G(\cosh^{-1}c) + G(-\cosh^{-1}c)\} \quad (4.11)$$

and

$$G(\lambda) = \frac{-a_0\{2\gamma_0(u_0-u_0^*)\,\kappa_+(u_0)\}^{-1}}{\kappa_-(\cos(\theta_0+i\lambda))\,(\cos(\theta_0+i\lambda)-u_0)}. \quad (4.12)$$

On using the identity (4.7), we find

$$p_e(\mathbf{x};t) = \mathrm{Re}\left\{\frac{1}{r_0}\sum_0^{\infty}\int_1^{\infty}\delta^{(n)}\left\{c - \frac{a_0 t - u_1(x+y)}{r_0}\right\}\left\{\frac{-iu_2(x-y)}{r_0}\right\}^n \frac{F(c)}{n!}\,dc\right\}, \quad (4.13)$$

which is non-zero provided that

$$a_0 t \geqslant r_0 + u_1(x+y) \quad (4.14)$$

and is zero otherwise. On formally integrating term by term and expanding the sum (4.13) it is found that

$$p_e(\mathbf{x};t) = \mathrm{Re}\left\{\frac{1}{r_0}\sum_0^{\infty}\frac{1}{n!}\left\{\frac{iu_2(x-y)}{r_0}\right\}^n F^{(n)}\left(\frac{a_0 t - u_1(x+y)}{r_0}\right)\right\} \quad (4.15)$$

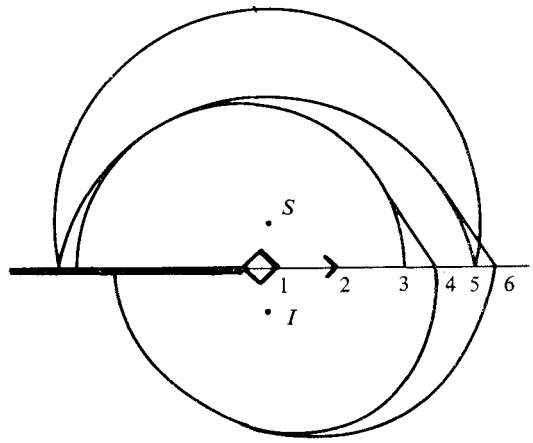


FIGURE 4. The wave fronts, in the initial-value problem, intersect the $x$ axis downstream of the plate edge, at the points where $x$ has the values (1) $u_1^{-1}(a_0t-r_0)$, (2) $x_0-y_0+u_1^{-1}a_0t$, (3) $a_0t-r_0$, (4) $(1+M)(a_0t-r_0)$, (5) $x_0+(a_0^2t^2-y_0^2)^{\frac{1}{2}}$, (6) $x_0+a_0t(1+M)-y_0(2M+M^2)^{\frac{1}{2}}$, where $u_1 \sim M^{-1}$ at low Mach number.

provided that the *inequality of* (4.14) holds; in this case the expression (4.15) is interpreted as the Taylor series of the ordinary function

$$p_e(\mathbf{x};t) = \mathrm{Re}\left\{\frac{1}{r_0}F\left(\frac{a_0t-u_1(x+y)+iu_2(x-y)}{r_0}\right)\right\}. \tag{4.16}$$

At the wave front, where $a_0t = r_0+u_1(x+y)$, formula (4.15) is not appropriate since the argument of $F^{(n)}$ equals unity, and (4.11) shows that $F(c)$ is singular at $c = 1$. On the front the solution is left as the ultradistribution (4.13). Bearing in mind that $p_e$ appears only for $\theta < \frac{1}{4}\pi$, this interpretation of the *edge scattered instability wave* $p_e$ suggests that it consists of a singular line $x+y = (a_0t-r_0)/u_1$, $x-y > 0$, $y > 0$, together with a 'tail' within the triangle bounded by $y = 0$, $x-y = 0$ and $x+y = (a_0t-r_0)/u_1$, wherein $p_e$ is given by (4.16). This contrasts with the other instability wave (figure 4), described by Jones & Morgan (1972), this consisting only of a singular line with no tail.

## 5. Description of the wave fronts

A precise description of the time-harmonic wave field is not feasible, on account of the complexity of the integral formulae for the various wave functions $\phi_\alpha$ described in §§ 2 and 3. The solution of the initial-value problem involves the additional task of evaluating the Fourier inversion integral (4.1), for each of these fields. Although this cannot be performed in detail, it is nevertheless possible to determine the *wave fronts* of these fields, and this information does give a useful insight into the nature of the solution.

Jones & Morgan (1972) have given such a description for the case of a doubly infinite vortex sheet [this solution corresponding to the function $\phi_v$ of the present

work, formula (3.11)] and show that the wave fronts in the stagnant fluid correspond to direct and reflected waves, together with a bow wave and instability wave (see figure 4).

Turning now to our diffracted wave $\phi_d$, given by formula (3.5), its Fourier inversion integral (4.1) has the form

$$p_d(\mathbf{x};t) = \int_{-\infty}^{\infty} d\tau \int_{-\infty}^{\infty} d\lambda\, E(\tau,\lambda) \int_{-\infty}^{\infty} \exp\left(ikr\cosh\tau + ikr_0\cosh\lambda - ika_0t\right) dk, \quad (5.1)$$

and $k$ appears only where shown explicitly. It is seen that the integrand is exponentially small in the upper half $k$ plane if

$$a_0t < r + r_0, \quad (5.2)$$

for any $\tau$ and $\lambda$, whence $p_d(\mathbf{x};t) = 0$ for these values of $t$, on collapsing the $k$ contour in the upper half-plane. The wave front clearly occurs on the circle

$$r = a_0t - r_0 \quad (5.3)$$

and the time $t = (r+r_0)/a_0$ is the time taken for a signal to travel, via the edge, from the source point $r_0$ to the observation point $r$.

The secondary bow wave $\phi_{2b}$, given by (3.15) for $\theta < \theta_M$, can be dealt with in a similar manner. For a given value of $s$ on the loop $L$ of formula (3.15), its contribution to the Fourier inversion integral (4.1) will first occur when

$$a_0t = -sx + i\gamma_s y + r_0, \quad -\cos\theta < s < -\cos\theta_M.$$

Thus the $s$ integral vanishes for all times such that

$$a_0t < r_0 + r\cos(\theta - \theta_M). \quad (5.4)$$

Since the bow wave $\phi_{2b}$ occurs only for $\theta < \theta_M$, the wave front at a given time $t$ ($> r_0/a_0$) is a straight line from $x = (1+M)(a_0t - r_0)$, $y > 0$, to the point of contact with the cylindrical diffracted wave front $r = a_0t - r_0$, and is shown in figure 4.

Our picture of the field in the stagnant fluid ($y > 0$) is completed by considering the edge instability wave $\phi_e$. Formula (4.8) shows that this field does not contribute until the time

$$a_0t = u_1(x+y) + r_0 \quad (5.5)$$

and is confined to the domain $\theta < \frac{1}{4}\pi$. Evidently the signal from $r_0$ travels to the edge (taking time $r_0/a_0$) and then induces a wave field in the triangular region bounded by the lines $x = y$ and $x+y = (a_0t - r_0)/u_1$, with $u_1 \sim 1/M$ at small Mach number $M$.

Finally, it is remarked that the field $\psi$ in the moving fluid ($y < 0$) can be dealt with by a similar procedure and will not be described in detail here. The double integral expression (2.46) has its paths deformed onto the hyperbolae

$$t = \cos(\theta_0 + i\lambda)$$

and

$$s = \{-\cos(\theta_2 + i\tau) + M\}(1-M^2)^{-1},$$

with polar co-ordinates $(r_2, \theta_2)$ defined by

$$x = (1-M^2)\, r_2\cos\theta_2, \quad y = -(1-M^2)^{\frac{1}{2}}\, r_2\sin\theta_2$$

(cf. Jones & Morgan 1972). On taking due account of possible pole and branch-point contributions entailed in the deformations, as in the analysis of § 3, the field is found to consist essentially of three components $\psi_v$, $\psi_d$ and $\psi_e$. The field $\psi_v$ is that appropriate to a doubly infinite vortex sheet, as discussed by Jones & Morgan (1972), and can be interpreted as a convected transmitted wave together with an instability wave. The function $\psi_d$ is a (convected) edge diffracted field and $\psi_e$ is an exponentially growing edge instability field, valid for angles $\theta$ that exceed a certain cut-off value $\theta = -\theta_c$. If the radical $\varpi$ [formula (2.17)] has the value

$$\varpi_0 = -\varpi_1 + i\varpi_2$$

when $u = u_0$, then the cut-off angle $\theta_c$ is found to have the value

$$\tan\theta_c = u_2/\varpi_1$$

and is given approximately by $\tan\theta_c \sim (1+2M)^{-1}$ when $M$ is small. In the initial-value problem, the wave front associated with $\psi_e$ is given by

$$u_1 x - \varpi_2 y = a_0 t - r_0,$$

whence

$$x - y \sim M(a_0 t - r_0)$$

for small values of $M$ (see figure 4).

## 6. Discussion

This paper has examined the simplest prototype problem incorporating the interaction between an acoustic source, an unstable shear layer, and the solid boundary from which the shear layer is shed. The primary instability field generated on a vortex sheet has been examined by Jones & Morgan (1972); the new feature of our work is the analysis of the coupling between the instability field and the large but inhomogeneous solid surface. This coupling produces an edge scattered instability wave (3.14), and contributes also a cylindrical diffracted field, the latter being the radiating part of $\phi - \hat{\phi}$, given by (2.49), proportional to the eigensolution $\phi_E$ given by (2.50). Because of this diffracted field, the instability of the vortex sheet is *not* decoupled from the acoustic field, as it is in the case of an infinite vortex sheet (Jones & Morgan 1972). There the instability wave is essentially a pseudo-sound field, which tends *uniformly* to its incompressible limit as $a_0 \to \infty$. The cylindrical diffracted field for large but finite $a_0$ is, on the other hand, close to the incompressible limit only when $kr \ll 1$ and *not* in the wave field. Thus, while in the case of an infinite vortex sheet one may, without damage to the acoustics, ignore instabilities or not according to one's conviction as to whether they are relevant to real turbulent flows at high Reynolds number, one cannot here ignore instabilities and leave the radiating acoustic field unchanged. Refer, for example, to (3.8) and (3.9), where the diffracted wave arising from the instability eigenfunction $\phi_E$ was shown to dominate the whole diffracted field if the source was within a hydrodynamic wavelength $U/\omega$ of the edge.

Now of course the model adopted here for the shear layer leads to a totally unphysical representation of the basic instabilities, even when the source excitation

is appropriately smoothed. For even at one fixed low frequency, at which one could argue the relevance of a vortex sheet model to describe the initial flow near the plate edge, the model predicts exponential growth downstream. In practice, at least three mechanisms are available to curtail the growth (Crow & Champagne 1971, p. 574), namely, the eddy-viscosity effect of small-scale background turbulence, the spreading of the mean flow, and the saturation resulting from nonlinear energy cascade. Although one can argue that downstream conditions in an elliptic problem might affect the flow near the edge, it is plausible to think that the flow near the edge (and hence the sound field arising from instability–edge coupling) can be calculated according to linear spatial growth theory *provided* that theory shows the effect of the edge to be insignificant at distances at which nonlinear or spreading effects must obviously be called into play. That is certainly the case here (Orszag & Crow 1970), and to some extent justifies our belief that the diffracted part of the instability field is correctly given by our analysis, regardless of the downstream conditions which must prevent us here from correctly describing the primary instabilities. (Crow (1972) has, however, given a *realistic* modelling of the primary instabilities on a round jet, and has shown that the sound field calculated from this model agrees well with the measured sound field of an externally excited high speed jet at angles around 40° to the exhaust, where one would expect the primary instabilities to dominate.)

In a forthcoming paper, we shall extend this work to the case of sound propagation out of a duct, with uniform mean flow within the duct and its continuation into a cylindrical vortex sheet. Many treatments have, of course, been given of the zero-flow case. No published work appears to deal with the case of different flow on the two sides of the duct wall, though the eigenfunctions [corresponding to $\phi_E$ of (2.50)] for that case have been examined (Crighton 1972*b*). At all frequencies these eigenfunctions have a forward directivity ($\tan \frac{1}{2}\theta$ at high and $(1-\cos\theta)^2$ at low frequencies, $\theta$ being zero in the downstream direction), whereas the directivity of the basic diffracted field, neglecting instabilities, is uniform at low frequencies and peaked in the rear arc ($\theta < \frac{1}{2}\pi$) at high frequencies. The question arises as to whether the eigenfunction ever dominates the basic diffracted field, when the two are coupled so as to ensure the kind of causality requirement discussed in the present paper. If it does, coupling between instabilities and a duct provides a means of generating intense forward-arc fields in a situation where neglect of instabilities would lead one to the conclusion (Crighton 1973) that sound generated within a duct can only be heard appreciably in the rear arc. We might call this process *parametric amplification* of internally generated sound by the unstable shear layer coupled to the duct. Further details will not be given here, nor will we do more than mention the possible relevance of parametric amplification to the noise fields of jet engines operating at low exhaust speeds.

D. G. Crighton acknowledges with thanks the support of a contract from the Ministry of Defence (Procurement Executive), administered by the National Gas Turbine Establishment, Pyestock, Hampshire.

## Appendix. The Wiener–Hopf kernel function

The kernel function $K(s)$ of formula (2.30) is

$$K(s) = (\varpi_s + \gamma_s D_s^2)/\varpi_s \gamma_s, \tag{A 1}$$

with $\varpi_s$, $\gamma_s$ and $D_s$ given by (2.16), (2.17) and (2.28); it has cuts from $s = 1$ to $s = \infty$ and from $s = -(1+M)^{-1}$ to $s = -\infty$.

To locate the zeros of $K(s)$, write the numerator of (A 1) in terms of $D_s = 1 + Ms$ and rationalize to get

$$(D_s^2 - 1)(D_s^2 + aD_s + 1)(D_s^2 + bD_s + 1) = 0 \tag{A 2}$$

at a zero, where $a$ and $b$ are the roots of the quadratic

$$x^2 + 2x - M^2 = 0.$$

On eliminating spurious roots introduced by the rationalization it is found that, for $M < 1$, the genuine roots of $K(s)$ are given by the complex conjugate numbers $u_0 = -u_1 + iu_2$ and $u_0^* = -u_1 - iu_2$, with

$$u_0 = M^{-1}\{\tfrac{1}{2}[-1-(1+M^2)^{\frac{1}{2}}] + \tfrac{1}{2}i[2+2(1+M^2)^{\frac{1}{2}} - M^2]^{\frac{1}{2}}\}, \tag{A 3}$$

positive roots being understood. The zeros can be expressed in the more convenient form

$$u_0 = -u_1 + iu_2 = -\cos(\tfrac{1}{4}\pi + i\tau_0) \tag{A 4}$$

and

$$u_0^* = -u_1 - iu_2 = -\cos(\tfrac{1}{4}\pi - i\tau_0), \tag{A 5}$$

where $\tau_0$ is the positive root of the equation

$$\cosh \tau_0 = [1 + (1+M^2)^{\frac{1}{2}}]/2^{\frac{1}{2}}M. \tag{A 6}$$

For small values of the Mach number $M$, the roots $u_0$ and $u_0^*$ are given approximately by

$$u_0, u_0^* = (1/M)(-1 \pm i). \tag{A 7}$$

It is to be noted that the kernel $K(s)$ does not depend on the wavenumber $k$, although the strip $S$ of analyticity of the Wiener–Hopf equation (2.31) is inclined at an angle $\alpha = \arg k$ to the real negative $s$ axis, and the 'plus' and 'minus' regions $R_\pm$ depend similarly on $\arg k$ (see figure 1). Evidently the zeros $u_0$ and $u_0^*$ both lie within $R_-$ if $\arg k$ is sufficiently close to $\frac{1}{2}\pi$, but $u_0$ lies in $R_+$ if $\arg k$ is close to zero, and $u_0^*$ lies in $R_+$ when $\arg k$ is close to $\pi$. To deal with all these cases it is convenient to subtract out the factors $s - u_0$ and $s - u_0^*$ by writing

$$K(s) = (s - u_0)(s - u_0^*)\kappa(s) \tag{A 8}$$

so that $\kappa(s)$ is analytic and free from zeros in the cut $s$ plane. It is convenient further to isolate the factor

$$M^2/\varpi_s = M^2/\varpi_+ \varpi_-, \tag{A 9}$$

with

$$\varpi_\pm = \{(1 \pm M)s \pm 1\}^{\frac{1}{2}}, \tag{A 10}$$

and the function $\kappa(s)$ can now be decomposed by the usual Cauchy integral procedure, to give

$$\kappa_{\pm}(s) = \frac{M}{\varpi_{\pm}(s)} \exp\left[\pm \frac{1}{2\pi i}\int_{\Gamma_\alpha} \frac{\ln\{\varpi(z)\kappa(z)/M^2\}}{z-s}dz\right], \tag{A 11}$$

with the integral along a contour $\Gamma_\alpha$ from $z = -\infty \times e^{-i\alpha}$ to $+\infty \times e^{-i\alpha}$ within the strip $S$. For $\kappa_+$, $s$ lies to the right of the contour, while for $\kappa_-$, $s$ lies to the left of the contour. Although the strip $S$ and contour $\Gamma_\alpha$ depend on $\alpha = \arg k$, the integrals (A 11) together with their analytic continuations serve to define functions $\kappa_\pm$ which are completely independent of $k$, and analytic except for branch cuts from $-(1+M)^{-1}$ to $-\infty$ for $\kappa_+$ and from $+1$ to $+\infty$ for $\kappa_-$. The estimates (2.36) follow at once from (A 11) and (2.35).

Our main interest lies in the approximate evaluation of the functions $\kappa_\pm$ when $M$ is small. These may be obtained in a rigorous manner from the Cauchy integrals (A 11), but a simpler method is to note that except in neighbourhoods of radius $M$ around the branch points, the kernel $K(s)$ may be approximated uniformly in $s$, as $M \to 0$, by

$$K(s) \sim \{1+(1+Ms)^2\}(s^2-1)^{-\frac{1}{2}},$$

so that

$$\kappa(s) \sim M^2(s^2-1)^{-\frac{1}{2}}$$

and has the trivial decomposition

$$\kappa_+(s) = AM(s+1)^{-\frac{1}{2}}, \quad \kappa_-(s) = A^{-1}M(s-1)^{-\frac{1}{2}}, \tag{A 12), (A 13}$$

where $A$ is arbitrary and is assigned the value $A = 1$. Near the branch points $K(s)$ can be approximated in a different way, though one which overlaps with the above, and again an immediate factorization can be achieved, this factorization matching (A 12) and (A 13) in an appropriate sense as $s$ recedes from a branch point.

## REFERENCES


Alblas, J. B. 1957 *Appl. Sci. Res.* A **6**, 237.

Crighton, D. G. 1972*a* *Aero. Res. Counc. Current Paper*, no. 1195.

Crighton, D. G. 1972*b* *J. Fluid Mech.* **56**, 683.

Crighton, D. G. 1973 *AGARD* CP-131 *Paper*, no. 14.

Crighton, D. G. & Leppington, F. G. 1973 *Proc. Roy. Soc.* A **335**, 313.

Crow, S. C. 1972 Acoustic gain of a turbulent jet. *Am. Phys. Soc. Meeting, Boulder, Colorado*, paper IE.6.

Crow, S. C. & Champagne, F. H. 1971 *J. Fluid Mech.* **48**, 547.

Jones, D. S. 1972 *J. Inst. Math. Applics.* **9**, 114.

Jones, D. S. & Morgan, J. D. 1972 *Proc. Camb. Phil. Soc.* **72**, 465.

Noble, B. 1958 *Methods Based on the Wiener–Hopf Technique*. Pergamon.

Orszag, S. A. & Crow, S. C. 1970 *Stud. Appl. Math.* **49**, 167.